



Effects of Incorporating Measured Leaf Optical Properties in Land Surface Models

Wenzong Dong¹, Hua Yuan^{1*}, Ruqing Zhang¹, Hongmei Li¹, Lina Huang¹, Siguang Zhu², Jingman Peng³ and Yongjiu Dai¹

¹Southern Marine Science and Engineering Guangdong Laboratory (Zhuhai), Guangdong Province Key Laboratory for Climate Change and Natural Disaster Studies, School of Atmospheric Sciences, Sun Yat-sen University, Zhuhai, China, ²School of Atmospheric Sciences, Nanjing University of Information Science and Technology (NUIST), Nanjing, China, ³Qingyuan Meteorological Administration, Qingyuan, China

OPEN ACCESS

Edited by:

Yuqing Wang,
University of Hawaii at Manoa,
United States

Reviewed by:

Zong-Liang Yang,
University of Texas at Austin,
United States
Bo Qiu,
Nanjing University, China

*Correspondence:

Hua Yuan
yuanh25@mail.sysu.edu.cn

Specialty section:

This article was submitted to
Atmospheric Science,
a section of the journal
Frontiers in Earth Science

Received: 04 February 2021

Accepted: 04 May 2021

Published: 26 May 2021

Citation:

Dong W, Yuan H, Zhang R, Li H,
Huang L, Zhu S, Peng J and Dai Y
(2021) Effects of Incorporating
Measured Leaf Optical Properties in
Land Surface Models.
Front. Earth Sci. 9:663917.
doi: 10.3389/feart.2021.663917

Leaf optical properties (LOPs, i.e., leaf reflectance and transmittance), as a fundamental property of vegetation, are a key parameter in the canopy radiative transfer process. LOPs have a direct impact on the surface solar radiation partition and further affect surface flux exchanges. Recent works have provided reliable LOP data and mentioned that notable differences exist between the prescribed LOP values in current land surface models and measured LOP values, especially in the near-infrared (NIR) band. To evaluate the effects of different LOP values in land surface modeling, we ran two land surface models (the Community Land Model and the Common Land Model) with their default prescribed and measured values to examine the differences in simulated surface radiation partitions and fluxes. Our analyses show that differences in LOP values can lead to a large discrepancy in albedo, radiation partition, sensible heat flux and net radiation simulations. By using the measured LOP values, in the boreal forest zone, Southeast China, and the eastern United States, both models have a significantly increased surface albedo in the NIR band, with the difference exceeding 10% during JJA. Thus, the measured LOP values can improve the negative albedo bias in the boreal forest zone during summertime. Moreover, both models simulate less net radiation with a maximum reduction of 11 W/m^2 when incorporating the measured LOP values. Therefore, the total sensible heat flux can be reduced by as much as 11 W/m^2 . The results of this study emphasize that different LOP values can have a considerable effect on the surface radiation budget and sensible heat flux simulations which need attention in land surface model development. However, in current offline simulations, the measured LOP values cause slight changes in land surface temperatures and gross primary productivity (GPP).

Keywords: leaf optical properties, canopy radiative transfer, albedo, energy balance, surface radiation partition, surface fluxes, net radiation, land surface model

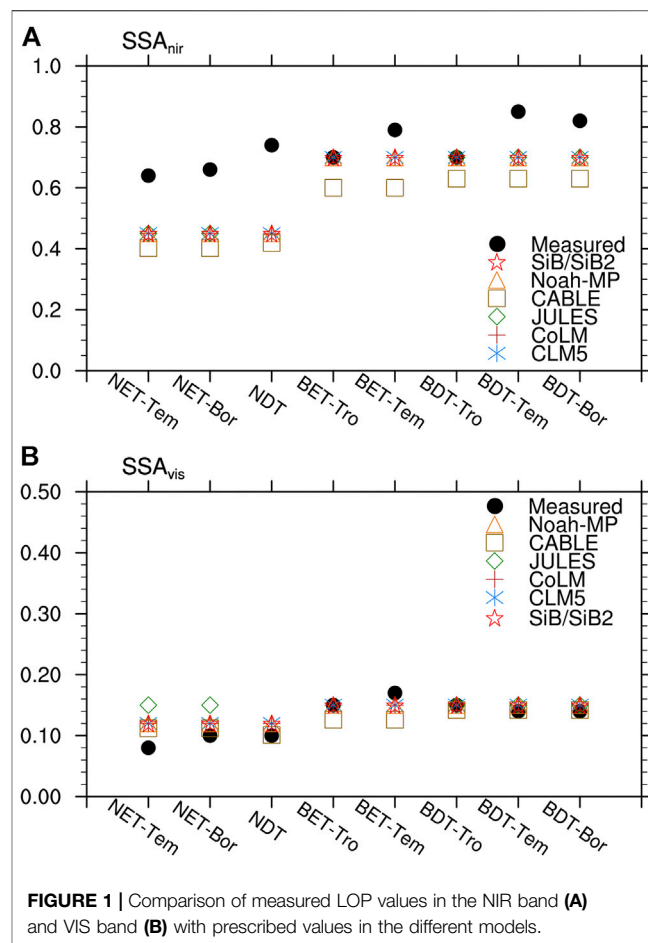
INTRODUCTION

Leaf optical properties (LOPs, i.e., leaf reflectance and transmittance) are among the most important driving factors of the Earth's surface energy balance. Reliable LOP data are also required for the parameterization of the two-stream transfer model (Dickinson, 1983; Sellers, 1985), which is widely adopted in land surface models (LSMs). Thus, LOPs can directly impact surface albedo, which is one

of the crucial parameters in the land surface radiation budget and energy balance (Zhai et al., 2014). Many kinds of studies also show that albedo plays an important role in land surface temperature change (Dickinson and Henderson-Sellers, 1988; Bounoua et al., 2002; Holland and Bitz, 2003; Winton, 2006) and has a significant effect on rainfall (Xue and Shukla, 1993; Dirmeyer and Shukla, 1996; Knorr et al., 2001; Levine and Boos, 2017). Feedbacks between albedo and climate are also critical for climate predictions (Pu and Dickinson, 2012; Kovenock and Swann, 2018). Thus, surface albedo shapes the Earth's climate and climate change (Soden and Held, 2006; Randall et al., 2007).

In LSMs, the LOP values are generally prescribed for two broad bands in the shortwave region, i.e., the visible band (VIS) and the near-infrared band (NIR), and for different land cover types or plant functional types (PFTs), such as needleleaf evergreen tree (NET), needleleaf deciduous tree (NDT), broadleaf evergreen tree (BET) and broadleaf deciduous tree (BDT). These PFTs can be further classified as tropical (Tro), temperate (Tem) and boreal (Bor) by broad geoclimatic zones. Many current LSMs (e.g., the Community Land Model (CLM), the Jena Scheme of Atmosphere Biosphere Coupling in Hamburg (JSBACH), and the Joint United Kingdom Land Environment Simulator (JULES)) either rely on the “time-invariant optical properties look-up table” of the Simple Biosphere (SiB) model presented 30 years ago by Dorman and Sellers (1989) or lack references for the properties they do employ (Majasalmi and Bright, 2019). By examining the prescribed single-scattering albedo [SSA, i.e., the sum of reflectance (α) and transmittance (τ)] values of CLM (Lawrence et al., 2019), CoLM (Dai et al., 2003; Dai et al., 2004; Ji and Dai, 2010), Noah-Multi parameterization LSM (Noah-MP; Niu et al., 2011), JULES (Clark et al., 2011), SiB/SiB2 (Dorman and Sellers, 1989) and the Community Atmosphere Biosphere Land Exchange model (CABLE; Haverd et al., 2018), as shown in **Figure 1**, SSA values are very close to each other and almost identical to those in the SiB/SiB2 model.

Recent work by researchers has provided LOP data through various kinds of methods. For example, LOPs can be measured by using optical instruments (Middleton and Sullivan, 2000; Göttlicher et al., 2011; Lukeš et al., 2013; Mottus et al., 2014; Hovi et al., 2017; Rautiainen et al., 2018), simulated by leaf-level modeling of LOP models (Jacquemoud and Baret, 1990; Malenovsky et al., 2007; Feret et al., 2008; Zhang et al., 2017) or retrieved by inversion of remote sensing data sets (Hagolle et al., 2005; Pinty et al., 2011; Verrelst et al., 2015). The reported LOP values from early literature (e.g., Goudriaan, 1977; Dickinson, 1983) are different from those in the listed models (**Figure 1**). More recently, Majasalmi and Bright (2019) used various spectral databases to synthesize and harmonize the key optical property information of the PFT classification shared by many leading LSMs and found notable differences between the CLM default and measured LOP values in the NIR band. The LOP values for different PFTs provided by Majasalmi and Bright (2019) are highlighted in **Figure 1** and referred to as “measured”. Except for tropical broadleaf trees (i.e., BET-Tro and BDT-Tro), the measured SSA values are generally 0.1–0.29 higher than the prescribed values in the NIR band (**Figure 1A**). The most



significant difference occurs for the needleleaf trees (i.e., NET-Tem, NET-Bor and NDT). In the VIS band, no difference greater than 0.04 is found (**Figure 1B**). Thus, Majasalmi and Bright (2019) suggested that NIR optical properties require an update.

To date, research has focused on the acquisition of LOP data. Although substantial work has been completed, these data have not been applied in LSMs. The effects of such a large difference in LOP values between prescribed model and measured values in model simulations are still unclear. To this end, in this study, we incorporate the measured LOP values, which are provided by Majasalmi and Bright (2019), in CLM5 and CoLM and compare the difference in simulated albedo as a result of changed LOP values. Moreover, we analyze the changes in surface radiation partition, surface fluxes, net radiation, and land surface temperatures. Finally, differences in simulated global annual gross primary productivity (GPP) are also compared.

MODELS AND EXPERIMENTS

Model Description

In this study, we use two widely adopted land surface models, the Community Model (CLM5) and the Common Land Model (CoLM2014), to conduct offline simulations. Both models

calculate radiative transfer through the canopy and the ground surface using the two-stream radiative transfer model. CLM5 is the latest version of the land component in the Community Earth System Model (CESM) (Danabasoglu et al., 2020) and builds on the progress made in CLM4.5. Lawrence et al. (2019) present an overview of model developments. More detailed descriptions can be found in the technical manual (Lawrence et al., 2018).

CoLM combines the advantages of three land surface models: NCAR LSM (Bonan, 1996; Bonan, 1998), Biosphere-Atmosphere Transfer Scheme (BATS) (Dickinson et al., 1993) and Institute of Atmospheric Physics LSM (IAP94) (Dai and Zeng, 1997). CoLM2014 (<http://globalchange.bnu.edu.cn/research/models>) is an update of CoLM2005 (Dai et al., 2004; Ji and Dai, 2010) and CoLM (Dai et al., 2003).

Experimental design

For the purpose of examining the effects of different LOP values on land surface modeling, we run offline simulations of CLM5 and CoLM2014 with their default LOP values (named CLM and CoLM) and with the measured LOP values (named CLM_{mLOP} and $CoLM_{mLOP}$) provided and suggested by Majasalmi and Bright (2019) (Table 1). The LOP values are given in different PFTs of CLM5 as an example. CoLM uses the “mosaic” approach to account for different land covers within a model grid cell. However, in contrast to PFT, CoLM2014 uses the land cover type classification to represent subgrid-scale heterogeneity. Therefore, the forest classification is slightly different from that of CLM5. To make the land cover type of CoLM2014 more consistent with that of CLM5, we map the forests of CoLM2014 by geoclimatic zones. That is, the needleleaf forest (i.e., NET and NDT) and broadleaf forest (i.e., BET and BDT) of CoLM2014 are further broken down to NET-Tem (NDT-Tem), NET-Bor (NDT-Bor), BET-Tro (BDT-Tro), BET-Tem (BDT-Tem) and BET-Bor (BDT-Bor). We consider the mixed forest of CoLM2014 as NET, which is mainly located in Canada. The land cover results of CLM5 and CoLM2014 are shown in Figure 2. After the new land cover mapping, the vegetation distribution of CoLM2014 is very close to that of CLM5; for example, needleleaf trees and BET are mainly distributed in the boreal forest zone and tropics, respectively.

Using the remotely sensed leaf area index, CLM and CLM_{mLOP} are simulated with default settings (except for the LOP values).

The component set in CLM is I2000Clm50Sp. Extension modes are not activated (e.g., biogeochemical cycles and carbon nitrogen cycling). Except for LOP values, CoLM and $CoLM_{mLOP}$ are both kept as the default settings. Ten-year simulations at a spatial resolution of $0.9^\circ \times 1.25^\circ$ for CLM (CLM_{mLOP}) and $0.5^\circ \times 0.5^\circ$ for CoLM2014 ($CoLM_{mLOP}$) are conducted. CRUNCEPv7 data are the climate forcing for both CLM5 and CoLM2014. The running time of these two models is 2000–2009. The first half of the decade (2000–2004) is considered as spin-up and the seasonal averages over the last five years (2005–2009) are compared and analyzed.

RESULTS

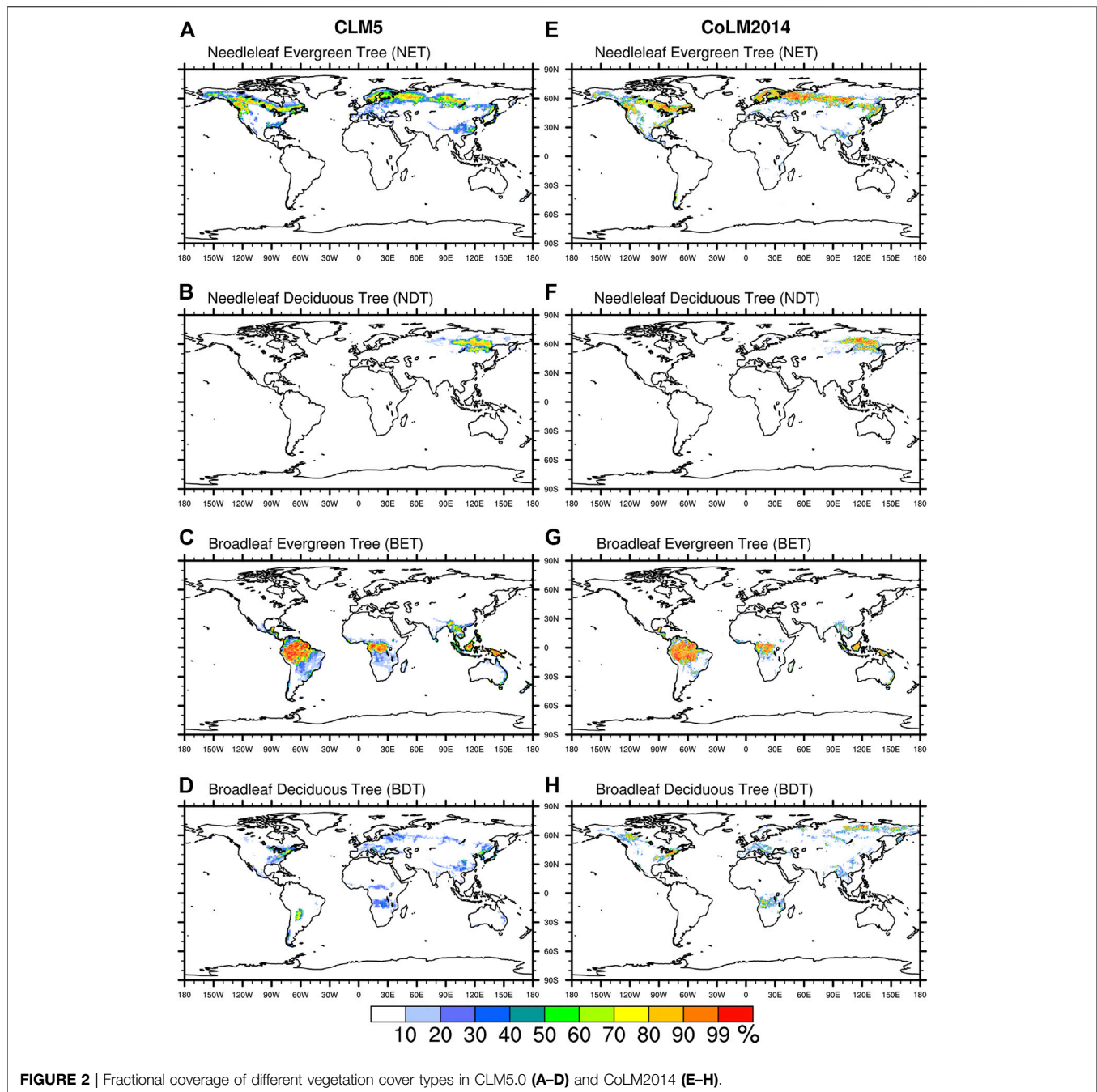
Albedo

We first compare the black-sky albedo in the NIR band simulated by CLM and CLM_{mLOP} (Figure 3). Their differences, which can be as much as 3%–10% in most regions, are mainly located in the boreal forest zone, Southeast China and the eastern United States, most notably in JJA (Figure 3C). These areas are typically associated with dense coniferous trees and broadleaf trees (Figure 2) with a large difference in τ_{nir} values, especially for NDT (the measured τ_{nir} value is 0.28 greater than that of prescribed values, Table 1). Therefore, in areas with a high proportion of NDT (more than 90%, Figure 2B), Figure 3C shows that the differences can exceed 10%. The differences in simulated albedo generally exhibit a strong seasonal dependence. That is, the difference increases substantially in the growing season (MAM and JJA) and decreases during the nongrowing season (DJF and SON). However, there are still many regions with 1–5% differences. The difference in LOP values is mainly in the NIR band (Figure 1 and Table 1). The difference in VIS band albedo is less than 1% (not shown). For white-sky albedo, the consequence is similar to that for black-sky albedo. Therefore, CLM_{mLOP} calculates all-sky albedo up to 1–5% greater than CLM in the abovementioned regions (not shown).

Figure 4 presents the difference in the black-sky albedo in the NIR band between CoLM and $CoLM_{mLOP}$. CoLM generally shows the same results as CLM. During MAM and JJA, the albedo increases by 3–10% in the boreal forest zone, Southeast China and the eastern United States. The differences also exceed 10% between CoLM and $CoLM_{mLOP}$ in areas with a high

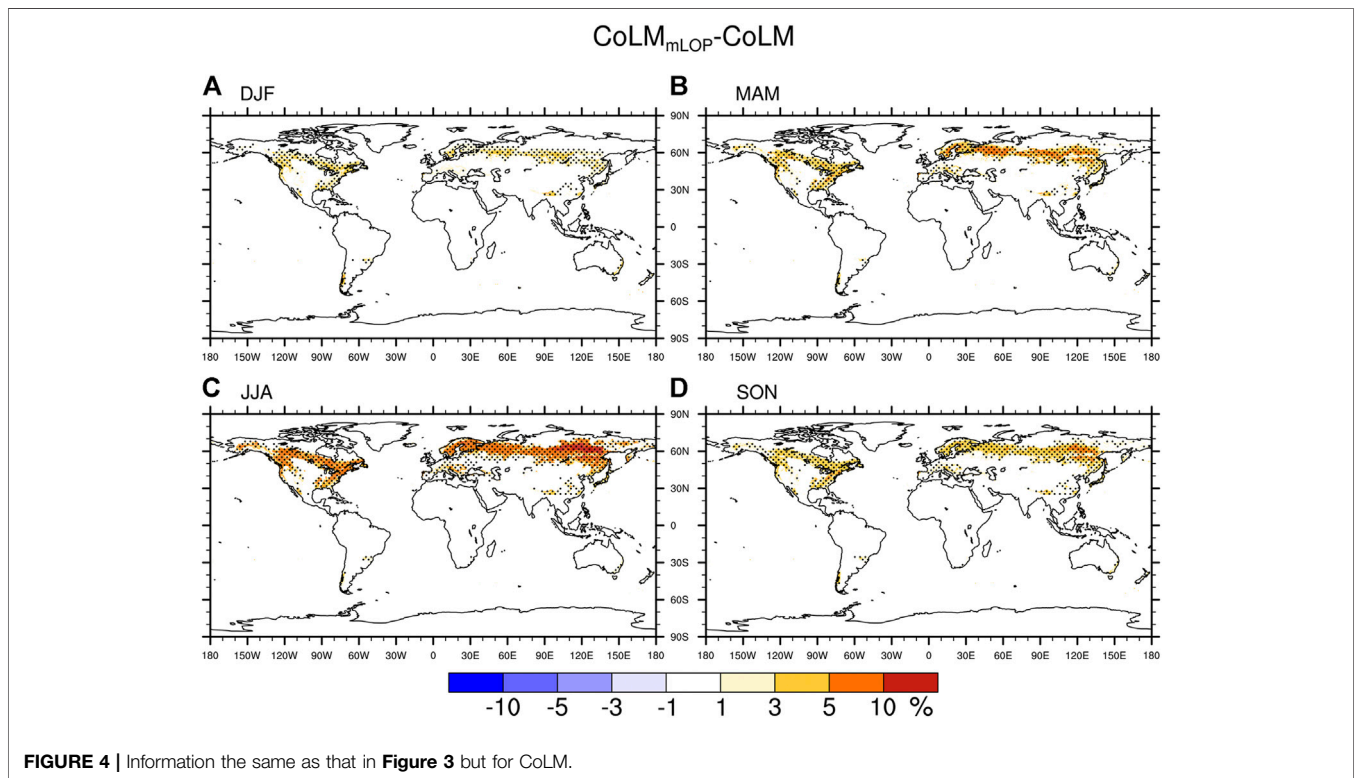
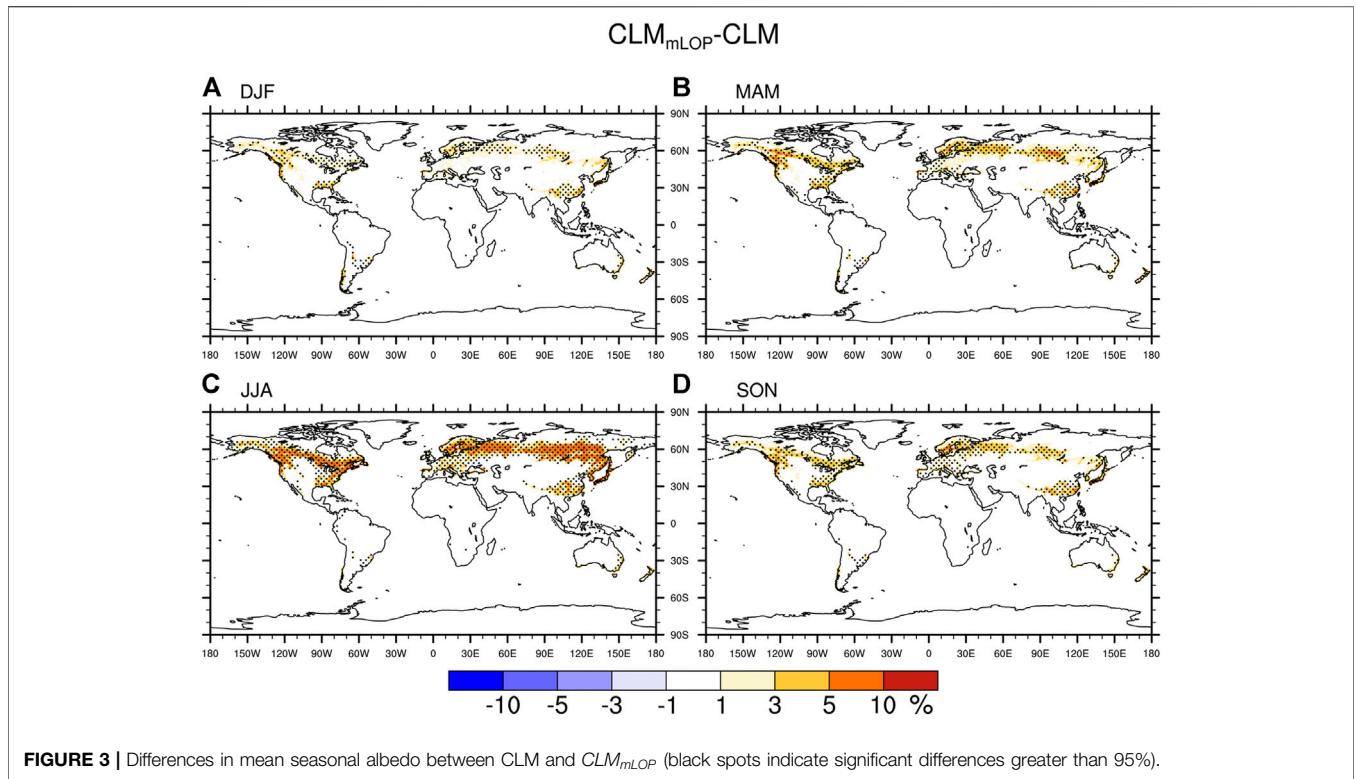
TABLE 1 | Default prescribed and measured leaf optical property values for each PFT set in CLM (CoLM) and CLM_{mLOP} ($CoLM_{mLOP}$).

Land cover type	CLM and CoLM				CLM_{mLOP} and $CoLM_{mLOP}$			
	Leaf reflectance (α)		Leaf transmittance (τ)		Leaf reflectance (α)		Leaf transmittance (τ)	
	NIR	VIS	NIR	VIS	NIR	VIS	NIR	VIS
NET-Tem	0.35	0.07	0.10	0.05	0.36	0.05	0.28	0.03
NET-Bor	0.35	0.07	0.10	0.05	0.37	0.06	0.29	0.04
NDT	0.35	0.07	0.10	0.05	0.36	0.06	0.38	0.04
BET-Tro	0.45	0.10	0.25	0.05	0.45	0.10	0.25	0.05
BET-Tem	0.45	0.10	0.25	0.05	0.46	0.11	0.33	0.06
BDT-Tro	0.45	0.10	0.25	0.05	0.45	0.10	0.25	0.05
BDT-Tem	0.45	0.10	0.25	0.05	0.42	0.08	0.43	0.06
BDT-Bor	0.45	0.10	0.25	0.05	0.40	0.09	0.42	0.05



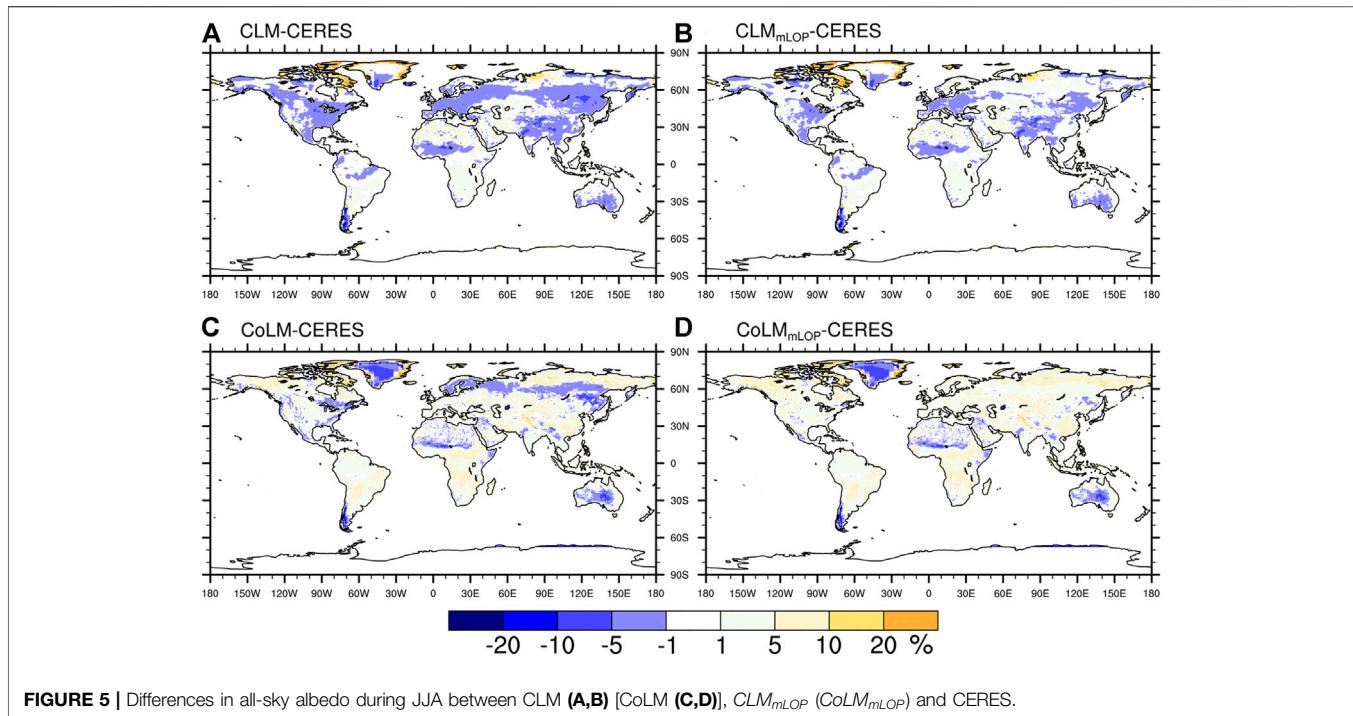
proportion of NDT (Figure 2F). Figures 4A,D also show that in comparison to CoLM, $CoLM_{mLOP}$ simulates albedo up to 1–5% more in similar regions during DJF and SON. Similar to that with CLM, in the VIS band, the difference is negligible. Therefore, the all-sky albedo of $CoLM_{mLOP}$ generally increases by 1–5% in the same regions as CLM. It should be noted that the difference in all-sky albedo can be as much as 8% during JJA in the NDT regions. This result is comparable to the uncertainty introduced by PFT distributions, which has an impact on the seasonal cycle of surface albedo in the boreal forest zone of up to 10% during JJA (Hartley et al., 2017; Georgievski and Hagemann, 2018).

We also compare the simulated albedo of each model with observations derived from CERES-EBAF data (Kato et al., 2013), which are applied for ILAMB (Collier et al., 2018). The CERES provides monthly albedo from 2000 to 2013 at a 0.5° spatial resolution. We use data from 2005–2009 and grid them to the CLM5 resolution in comparison to the CLM and $CoLM_{mLOP}$. The monthly average all-sky albedo of CLM (CoLM) and $CoLM_{mLOP}$ are obtained from the ratio of monthly average total reflected shortwave radiation flux to incident shortwave radiation flux, and the same is true of CERES data. When comparing CLM and CoLM (Figures 5A,C), it is apparent from Figures 5B,D that



negative albedo bias can be significantly improved in the boreal forest zone during JJA. The driving forces behind this change are an increase in the NIR band albedo of *CLM_{mLOP}* and *CoLM_{mLOP}*.

This scenario suggests that the bias arising from model parameterizations can be compensated by LOP value adjustments.



Energy Partition and Surface Fluxes

Figures 6A,D show the differences in the zonal average reflected solar radiation between CLM (CoLM) and CLM_{mLOP} ($CoLM_{mLOP}$). Owing to the higher SSA_{nir} values of CLM_{mLOP} and $CoLM_{mLOP}$ (**Figure 1** and **Table 1**), the reflected solar radiation has a significant increase between 40° – 60° N and 30° – 55° S. The maximum increment occurs in JJA and can be as much as $6 W/m^2$. During DJF at 40° S, in comparison to CLM and CoLM, CLM_{mLOP} and $CoLM_{mLOP}$ simulate the surface-reflected radiation up to more than $3 W/m^2$. There are still noticeable differences (approximately 1 – $3 W/m^2$) during the other seasons.

LOP values can also directly influence the energy partition between the canopy and ground. Differences in the zonal average solar radiation absorbed by vegetation and the ground between CLM (CoLM) and CLM_{mLOP} ($CoLM_{mLOP}$) are shown in **Figures 6B,E**. CLM_{mLOP} and $CoLM_{mLOP}$ both show a considerable reduction in vegetation absorption (approximately 2 – $8 W/m^2$) between 40° and 60° N during JJA. This is due to the higher measured τ_{nir} values of coniferous trees and broadleaf trees than that of prescribed values (**Table 1**) that contribute to reducing light interception by the canopy. The differences between CoLM and $CoLM_{mLOP}$ can be as much as $10 W/m^2$ at 60° N. For the same reason, in the Southern Hemisphere, CLM_{mLOP} and $CoLM_{mLOP}$ calculate vegetation absorption at values less than those in CLM and CoLM by as much as $5 W/m^2$ during DJF. A higher τ_{nir} leads to a decrease in vegetation light interception, and more solar radiation penetrates vegetation and reaches the ground. At 60° N, CLM_{mLOP} and $CoLM_{mLOP}$ increase the ground absorption by up to $3 W/m^2$ during JJA. However, relatively small differences are found during the other seasons.

The changes in radiation partition lead to a difference in the sensible heat (SH) flux of vegetation and the ground (**Figure 6C**

and **Figure 6F**). There is a significant positive correlation between solar radiation absorption (**Figures 6B,E**) and SH (**Figures 6C,F**). The difference in SH is also mainly located between 40° – 60° N and 30° – 55° S. As shown in **Figures 6C,F**, at 60° N, CLM_{mLOP} and $CoLM_{mLOP}$ simulate vegetation SH up to $6 W/m^2$ higher than that in CLM and CoLM during JJA. In the Southern Hemisphere at 25 – 50° S, CLM_{mLOP} and $CoLM_{mLOP}$ have a lower vegetation SH than CLM and CoLM by as much as 1 – $3 W/m^2$. The differences between CLM and CLM_{mLOP} can exceed $4 W/m^2$ during DJF. There is a slight increase in ground SH, which is less than $1 W/m^2$.

It should be noted that the LOP uncertainty has a considerable effect on the total SH (**Figure 7**). The most obvious change is in the growing season. Therefore, we only show the differences during MAM and JJA. Due to the significant reduction in vegetation absorption for CLM_{mLOP} and $CoLM_{mLOP}$, the results show that the total surface SH of CLM_{mLOP} and $CoLM_{mLOP}$ can be reduced by 1 – $10 W/m^2$ in the boreal forest, Southeast China and the eastern United States during JJA. Especially in the NDT regions (**Figures 2B,F**), the differences can exceed $10 W/m^2$. Moreover, there are still 1 – $5 W/m^2$ differences in many regions during MAM. Thus, incorporating measured LOP values may overcome the problem of higher SH during the growing season of CLM (Burakowski et al., 2018). No significant differences (less than $1 W/m^2$ in most regions) in total latent heat are found.

Net radiation, land surface temperature and photosynthesis

As shown in **Figure 8**, it is apparent that CLM_{mLOP} and $CoLM_{mLOP}$ have much lower net radiation (R_n) (3 – $10 W/m^2$) than CLM and CoLM in the boreal forest zone, Southeast China and the eastern United States during JJA. This result is mainly due

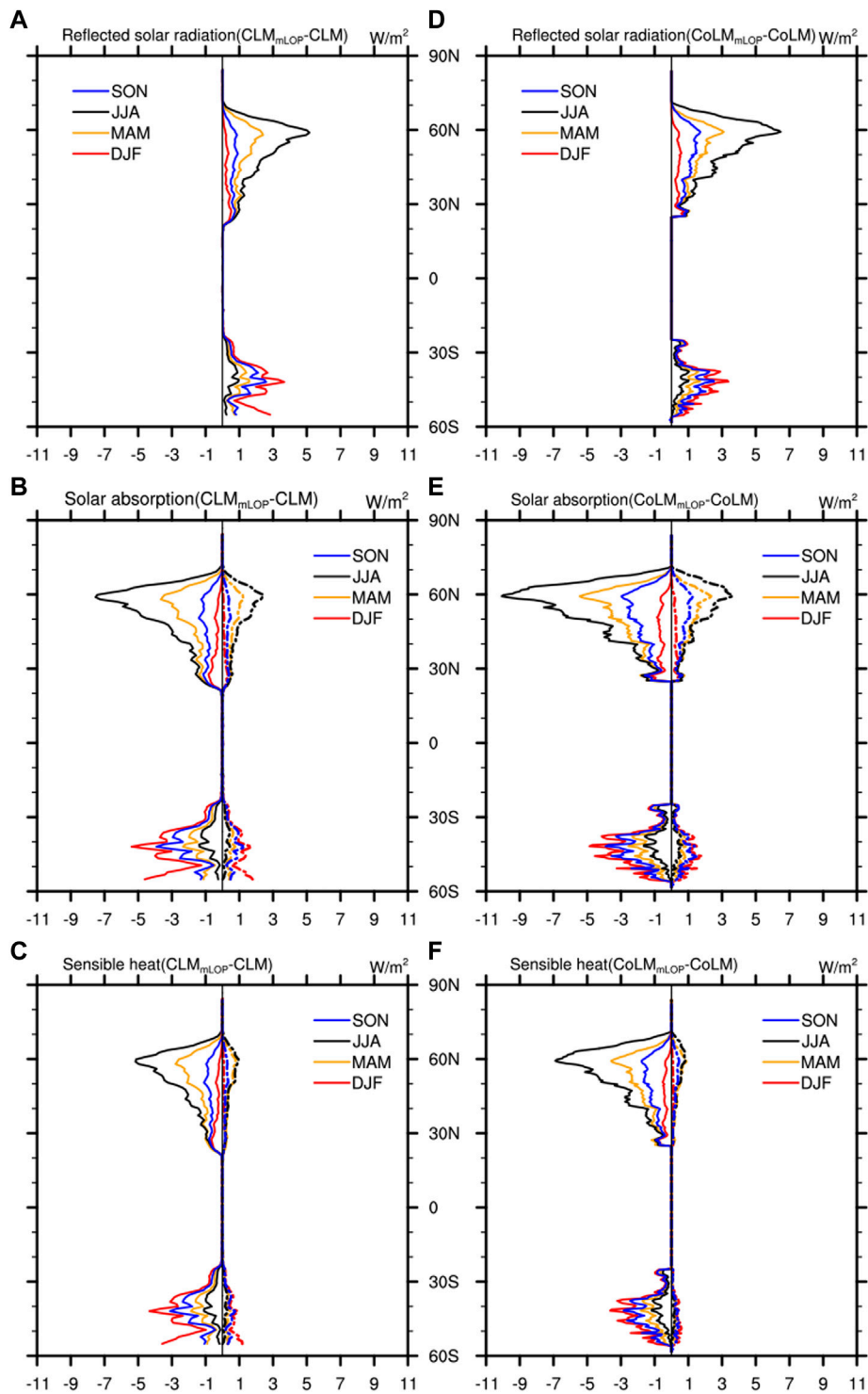
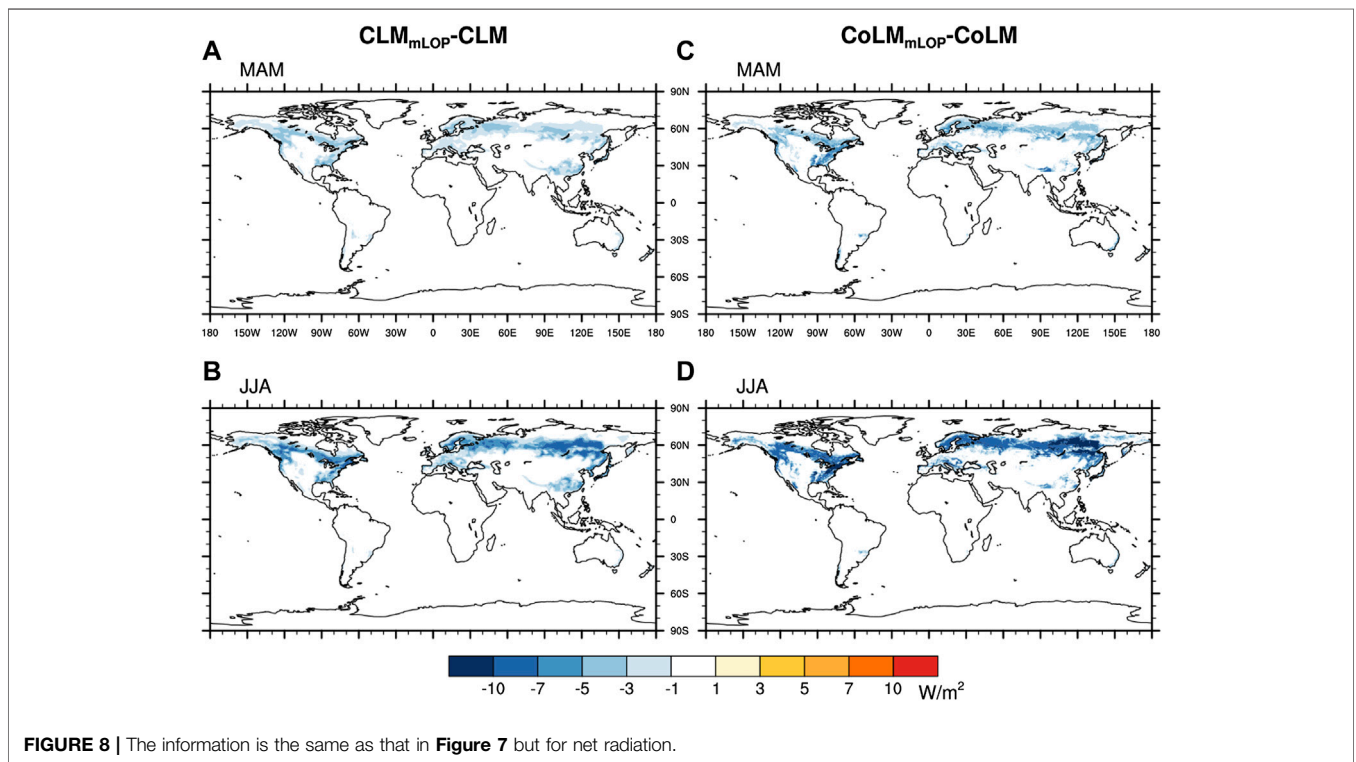
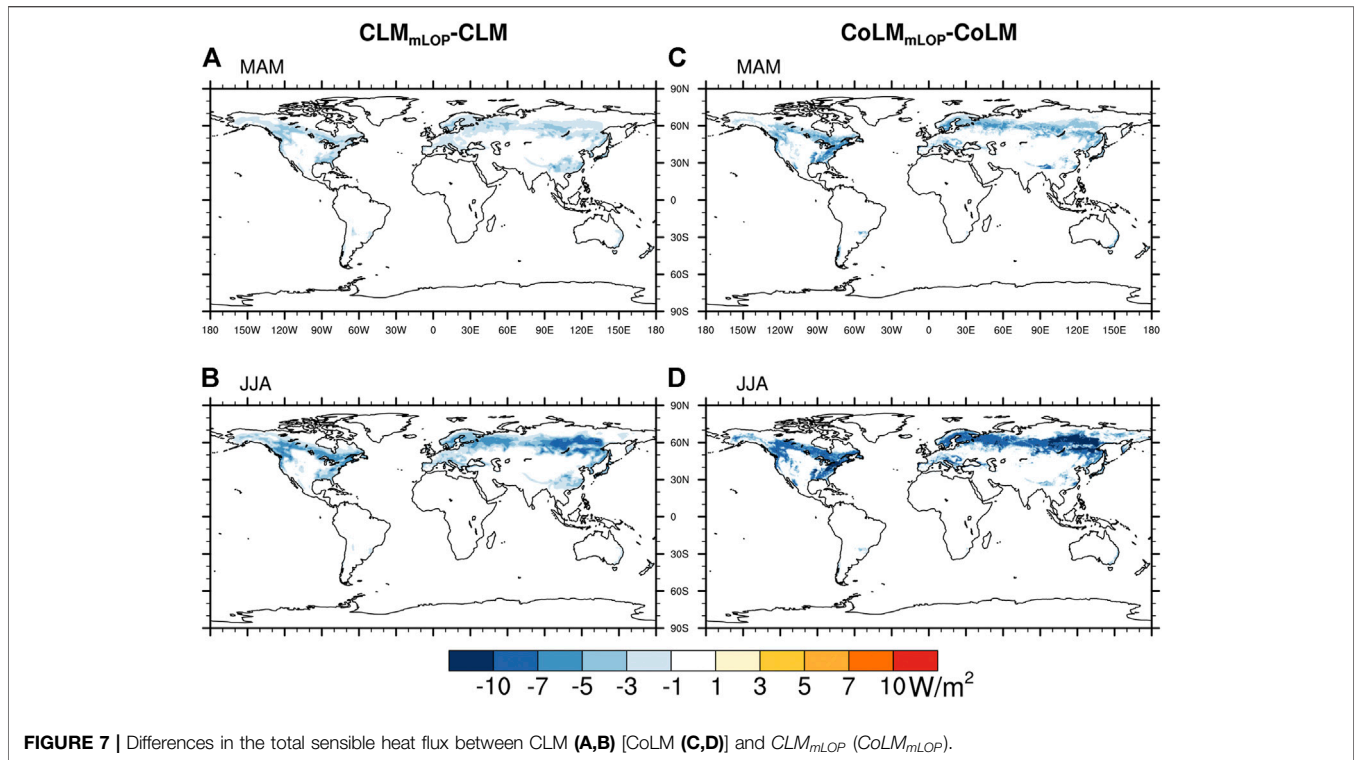


FIGURE 6 | Zonal average differences in reflected solar radiation (A,D), solar absorption (B,E) and sensible heat flux (C,F) between CLM (CoLM) and CLM_{mLOP} (CoLM_{mLOP}). The solid line and dashed line in **Figure 6B,C** and **Figure 6E,F** represent vegetation and the ground, respectively.

to the lower vegetation solar absorption in CLM_{mLOP} and CoLM_{mLOP} (Figures 6B,E). Moreover, the difference can be as much as 11 W/m² less in the NDT regions. During MAM, CLM_{mLOP} and CoLM_{mLOP} generally simulate R_n at 1–7 W/m² less than that in the

abovementioned regions. Notably, no significant changes in net infrared radiation are found when compared with net shortwave radiation. Therefore, the driving force behind the R_n change is a decrease in shortwave radiation absorption.



We also compared the differences in 2 m air temperature, ground (vegetation) temperature and skin temperature (i.e., radiative temperature). In both CLM and CoLM, “2 m” is defined as 2 m above the apparent sink for sensible heat (Dai

et al., 2001; Lawrence et al., 2018). **Figure 9** shows the differences in the land surface temperature between CLM (CoLM) and CLM_{mLOP} ($CoLM_{mLOP}$). Although the measured LOP values lead to a lower R_n , the 2 m air temperature has small changes

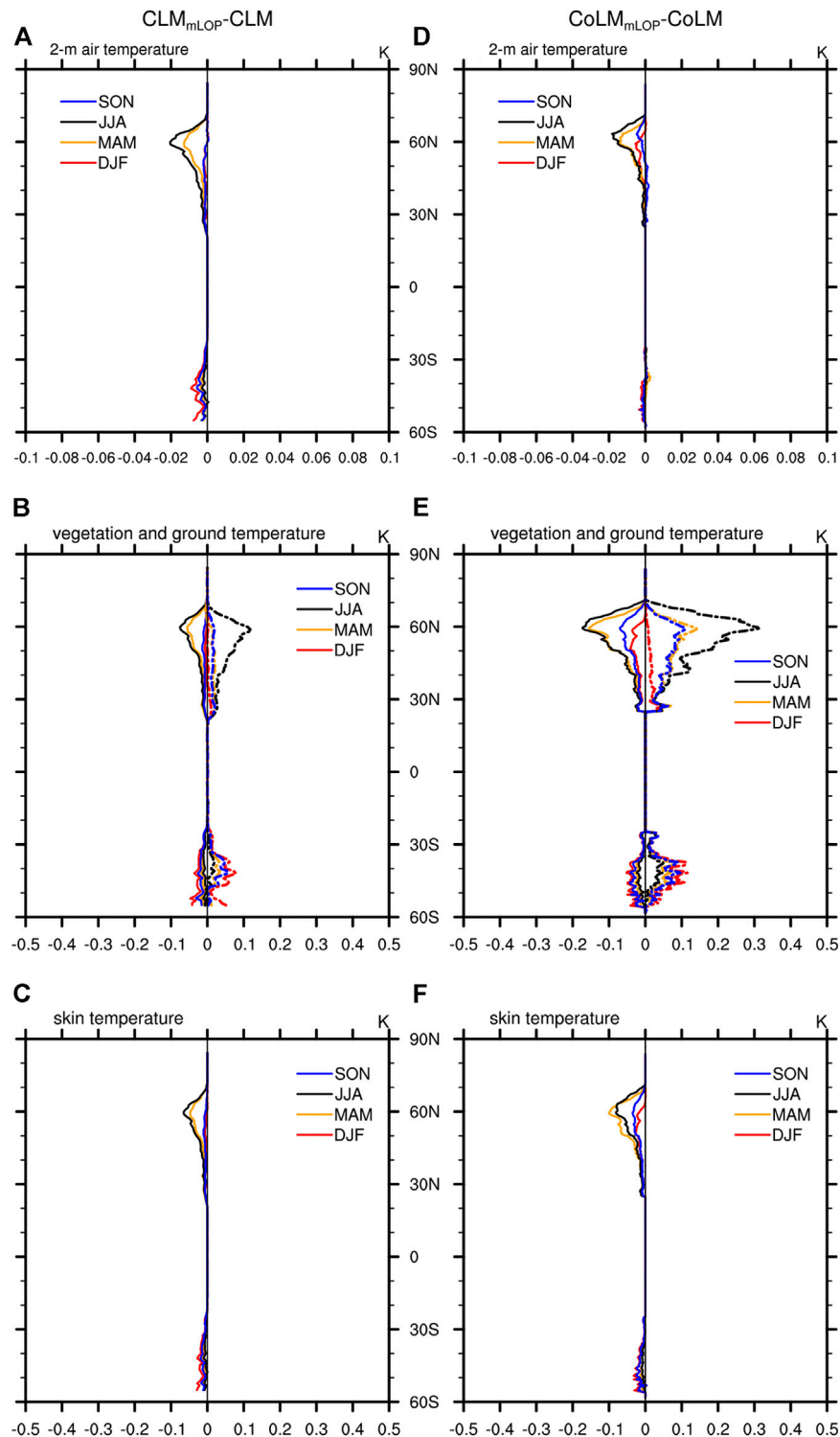


FIGURE 9 | Zonal average differences in 2-m air temperature (A,D), vegetation (ground) temperature (B,E) and skin temperature (C,F) between CLM (CoLM) and CLM_{mLOP} (CoLM_{mLOP}). The solid line and dashed line in (B,C,E,F) represent vegetation and the ground, respectively.

in current offline simulations. Compare to CLM and CoLM, the 2 m air temperature of CLM_{mLOP} and CoLM_{mLOP} only decreased by 0.01–0.02K between 40° and 60°N during JJA (Figures 9A,D). And during MAM, the differences between CLM (CoLM) and

CLM_{mLOP} (CoLM_{mLOP}) are less than 0.01K in most regions. Although the measured LOP values have a higher τ_{nir} which leads to an increase (reduction) in the ground (vegetation) absorption (Figures 6B,E), there are few effects on ground

and vegetation temperature. As shown in **Figure 9B**, CLM_{mLOP} has a higher ground temperature by only 0.1–0.11K than CLM between 40° and 60°N during JJA. And in the Southern Hemisphere, there are about 0.08K differences during DJF. Moreover, due to higher τ_{nir} contributes to reducing light interception by the canopy, the measured LOP values result in a lower vegetation radiation absorption. Therefore, CLM_{mLOP} simulates the vegetation temperature up to 0.07K lower than CLM at 60°N. For the same reason, CoLM shows a similar result as CLM. However, perhaps because CoLM takes no account of the effect of stem, the differences in ground and vegetation temperature between CoLM and $CoLM_{mLOP}$ can be as much as 0.3K and 0.17K at 60°N (**Figure 9E**), respectively. The measured LOP values also have few effects on the skin temperature. The skin temperature of CLM_{mLOP} can be lower by 0.04–0.065K than CLM between 40° and 60°N during JJA and MAM (**Figure 9C**). CoLM also shows the same result (**Figure 9F**). And for GPP, because the measured LOP and model prescribed values are very close in the VIS band (**Figure 1B**), there are slight changes in absorbed photosynthetically active radiation. Thus, the measured LOP values do not cause obvious changes in GPP simulations. The annual GPP calculated by CLM_{mLOP} and $CoLM_{mLOP}$ can only be 0.054 $Pg\ C\ yr^{-1}$ (0.03%) and 0.041 $Pg\ C\ yr^{-1}$ (0.02%) higher than that calculated by CLM and CoLM (not shown), respectively.

DISCUSSION AND CONCLUSIONS

By examining the prescribed LOPs of 6 LSMs, it was found that there is a difference of 0.1–0.29 from the measured SSA. The effects of such a large difference in LOP values between the prescribed model values and measured values of land surface modeling are still unclear. To determine the effects, we employed two widely used land surface models (CLM5 and CoLM2014) to examine the potential effects by incorporating the measured LOP values. The results indicate that the measured LOP values have a significant effect on surface albedo simulation, radiation partitioning and SH exchange in the boreal forest zone, Southeast China and the eastern United States. By using the measured LOP values, the surface albedo in the NIR band increases by 3–10% in the abovementioned regions, especially in JJA. Thus, the negative bias of surface albedo between the model and observational data can be significantly improved in the boreal forest zone during JJA. The energy partition can also be directly influenced by the LOP values. Both models generally have increased ground radiation absorption and less canopy radiation absorption. The measured LOP values also have a considerable effect on the net radiation and SH calculation. The net radiation of CLM_{mLOP} and $CoLM_{mLOP}$ decrease by 3–11 W/m^2 during JJA. Moreover, CLM_{mLOP} and $CoLM_{mLOP}$ show a 3–11 W/m^2 reduction in total SH during JJA. The results of this study emphasize that different LOP values can have a considerable effect on the surface radiation budget and SH simulations. It needs to be noted that all the comparisons in this study are monthly average which includes both daytime and nighttime. Since the solar radiative transfer process only happens in the day, the difference due to the modification of LOPs supposes to be

more pronounced if only the daytime is considered. However, the measured LOP values have few effects on 2 m air temperature. Perhaps this has something to do with the fact that we only did offline simulations. The 2 m air temperature of CLM_{mLOP} and $CoLM_{mLOP}$ only decreased by 0.01–0.02K. The measured LOP values also have few effects on ground (vegetation) temperature and skin temperature. As we mentioned above, due to the prescribed LOP values fell within the range of measured values in the VIS band, the GPP simulations also do not change obviously.

The measured LOP values provided by Majasalmi and Bright (2019) may not be “correct” per se. However, compared with the LOP values used in today’s LSMs, these data synthesize various observational data and spectral databases (Majasalmi and Bright, 2019). The purpose of this study is not to identify which optical parameter is the “correct” or better but to examine the effects of LOP values on surface radiation transfer and flux exchanges. As demonstrated from the results, LOP values could induce large uncertainties. In recent years, LSMs have aimed to develop more accurate and realistic physical processes. As a 1-D vertical canopy structure model, the two-stream model uses the fixed LOP values from a look-up table of “time-invariant” optical properties. It should be noted that LOPs generally show seasonal changes with vegetation growth and senescence stages (Yuan et al., 2017). In the future, a database of optical property data of tree species will be developed. These data could be used to realistically describe vegetation properties in LSMs to improve the accuracy of the model simulations. On the other hand, the two-stream model may be unrealistic in its assumption of the canopy structure and may introduce a large bias. In LSMs, the representation of canopy processes is given by the “big-leaf” model, which replaces the entire canopy with a single vegetation element regardless of the canopy profile (McGrath et al., 2016). However, different vegetation canopies may coexist and form multiple canopy layers, and significant three-dimensional canopy structures may exist (Yuan et al., 2014). And due to the non-linear response of photosynthesis, it is difficult to find a single value of leaf physiological properties to adequately represent the entire canopy under all conditions (McGrath et al., 2016). The shortwave radiation absorbed for photosynthesis is also used in the calculation of the energy budget. Therefore, using multilayer radiation transfer models to accurately describe the process of photosynthesis and radiation transfer within the canopy is the principal direction of current research and progress has already been made (Yuan et al., 2014; McGrath et al., 2016; Qiu et al., 2016). Yuan et al. (2014) developed a three-layer canopy radiation transfer model based on the three-dimensional structural canopy effect. McGrath et al. (2016) presented a multi-level radiation transfer scheme for the ORganising Carbon and Hydrology In Dynamic Ecosystems. And Qiu et al. (2016) developed a generalized radiative transfer scheme with nonuniform optical properties of adaxial and abaxial leaf surfaces and the nonuniform canopy structure in the vertical direction. In these researches, the radiation transfer model usually has more complex and realistic assumptions and shows a good improvement in some cases. In this study, we only operated offline simulations and found that LOP has a considerable impact

on model simulation, such as albedo simulation. However, albedo is important not only in LSMs but also in land-atmosphere interaction and coupling models (Betts, 2000; Betts, 2001; Berbet and Costa, 2003; Boisier et al., 2012). Therefore, the effects of LOP values on coupled land-atmosphere model simulations are also worth considering.

DATA AVAILABILITY STATEMENT

Publicly available datasets were analyzed in this study. This data can be found here: CERES albedo: <http://redwood.ess.uci.edu/mingquan/www/ILAMB/>

AUTHOR CONTRIBUTIONS

HY and YD contributed to the conception and design of the study. WD and LH performed the model simulation. WD

REFERENCES

- Berbet, M. L. C., and Costa, M. H. (2003). Climate Change after Tropical Deforestation: Seasonal Variability of Surface Albedo and its Effects on Precipitation Change. *J. Clim.* 16 (12), 2099–2104. doi:10.1175/1520-0442(2003)016<2099:CCATDS>2.0
- Betts, R. A. (2000). Offset of the Potential Carbon Sink from Boreal Forestation by Decreases in Surface Albedo. *Nature*. 408 (6809), 187–190. doi:10.1038/35041545
- Betts, R. (2001). Biogeophysical Impacts of Land Use on Present-Day Climate: Near-Surface Temperature Change and Radiative Forcing. *Atmos. Sci. Lett.* 2 (1-4), 39–51. doi:10.1006/asle.2001.0023
- Boisier, J. P., de Noblet-Ducoudré, N., Pitman, A. J., Cruz, F. T., Delire, C., van den Hurk, B. J. J. M., et al. (2012). Attributing the Impacts of Land-Cover Changes in Temperate Regions on Surface Temperature and Heat Fluxes to Specific Causes: Results from the First LUCID Set of Simulations. *J. Geophys. Res.* 117, D12116. doi:10.1029/2011jd017106
- Bonan, G. B. (1996). *Land Surface Model (LSM Version 1.0) for Ecological, Hydrological, and Atmospheric Studies: Technical Description and Users Guide. Technical Note.* Boulder, CO, United States: National Center for Atmospheric Research.
- Bonan, G. B. (1998). The Land Surface Climatology of the NCAR Land Surface Model Coupled to the NCAR Community Climate Model. *J. Clim.* 11 (6), 1307–1326. doi:10.1175/1520-0442(1998)011<1307:TLSCOT>2.0
- Bounoua, L., DeFries, R., Collatz, G. J., Sellers, P., and Khan, H. (2002). Effects of Land Cover Conversion on Surface Climate. *Climatic Change*. 52 (1-2), 29–64. doi:10.1023/A:1013051420309
- Burakowski, E., Tawfik, A., Ouimette, A., Lepine, L., Novick, K., Ollinger, S., et al. (2018). The Role of Surface Roughness, Albedo, and Bowen Ratio on Ecosystem Energy Balance in the Eastern United States. *Agric. For. Meteorology*. 249, 367–376. doi:10.1016/j.agrformet.2017.11.030
- Clark, D. B., Mercado, L. M., Sitch, S., Jones, C. D., Gedney, N., Best, M. J., et al. (2011). The Joint UK Land Environment Simulator (JULES), Model Description - Part 2: Carbon Fluxes and Vegetation Dynamics. *Geosci. Model. Dev.* 4 (3), 701–722. doi:10.5194/gmd-4-701-2011
- Collier, N., Hoffman, F. M., Lawrence, D. M., Keppel-Aleks, G., Koven, C. D., Riley, W. J., et al. (2018). The International Land Model Benchmarking (ILAMB) System: Design, Theory, and Implementation. *J. Adv. Model. Earth Syst.* 10 (11), 2731–2754. doi:10.1029/2018MS001354
- Dai, Y., Dickinson, R. E., and Wang, Y.-P. (2004). A Two-Big-Leaf Model for Canopy Temperature, Photosynthesis, and Stomatal Conductance. *J. Clim.* 17 (12), 2281–2299. doi:10.1175/1520-0442(2004)017<2281:ATMFC>2.0.CO
- Dai, Y. J., Zeng, X., and Dickinson, R. E. (2001). *The Common Land Model (CLM): Technical Documentation and User's Guide.* Atlanta, GA: Georgia Institute of Technology.
- Dai, Y., and Zeng, Q. (1997). A Land Surface Model (IAP94) for Climate Studies Part I: Formulation and Validation in Off-Line Experiments. *Adv. Atmos. Sci.* 14 (4), 433–460. doi:10.1007/s00376-997-0063-4
- Dai, Y., Zeng, X., Dickinson, R. E., Baker, I., Bonan, G. B., Bosilovich, M. G., et al. (2003). The Common Land Model. *Bull. Am. Meteorol. Soc.* 84 (8), 1013–1024. doi:10.1175/BAMS-84-8-1013
- Danabasoglu, G., Lamarque, J. F., Bacmeister, J., Bailey, D. A., DuVivier, A. K., Edwards, J., et al. (2020). The Community Earth System Model Version 2 (CESM2). *J. Adv. Model. Earth Syst.* 12 (2), e2019MS001916. doi:10.1029/2019ms001916
- Dickinson, R. E., Henderson-Sellers, A., and Kennedy, J. (1993). *Biosphere-atmosphere transfer scheme (BATS) version 1e as coupled to the NCAR community climate model.* Technical Note NCAR/TN-387+STR. Boulder, CO: National Center for Atmospheric Research. doi:10.5065/D67W6959
- Dickinson, R. E., and Henderson-Sellers, A. (1988). Modelling Tropical Deforestation: A Study of GCM Land-Surface Parametrizations. *Q. J. R. Met. Soc.* 114 (480), 439–462. doi:10.1002/qj.49711448009
- Dickinson, R. E. (1983). Land Surface Processes and Climate-Surface Albedos and Energy Balance. *Adv. Geophys.* 25, 305–353. doi:10.1016/s0065-2687(08)60176-4
- Dirmeyer, P. A., and Shukla, J. (1996). The Effect on Regional and Global Climate of Expansion of the World's Deserts. *Q. J. R. Met. Soc.* 122 (530), 451–482. doi:10.1002/qj.49712253008
- Dorman, J. L., and Sellers, P. J. (1989). A Global Climatology of Albedo, Roughness Length and Stomatal Resistance for Atmospheric General Circulation Models as Represented by the Simple Biosphere Model (SiB). *J. Appl. Meteorology Climatology*. 28 (19), 833–855. doi:10.1175/1520-0450(1989)028<0833:agcoar>2.0.co;2
- Feret, J.-B., François, C., Asner, G. P., Gitelson, A. A., Martin, R. E., Bidet, L. P. R., et al. (2008). PROSPECT-4 and 5: Advances in the Leaf Optical Properties Model Separating Photosynthetic Pigments. *Remote Sensing Environ.* 112 (6), 3030–3043. doi:10.1016/j.rse.2008.02.012
- Georgievski, G., and Hagemann, S. (2018). Characterizing Uncertainties in the ESA-CCI Land Cover Map of the Epoch 2010 and Their Impacts on MPI-ESM Climate Simulations. *Theor. Appl. Climatol* 137 (1-2), 1587–1603. doi:10.1007/s00704-018-2675-2
- Göttlicher, D., Albert, J., Naus, T., and Bendix, J. (2011). Optical Properties of Selected Plants from a Tropical Mountain Ecosystem - Traits for Plant Functional Types to Parametrize a Land Surface Model. *Ecol. Model.* 222 (3), 493–502. doi:10.1016/j.ecolmodel.2010.09.021

FUNDING

This research is supported by the National Key R&D Program of China (Grant No. 2017YFA0604300), Natural Science Foundation of China (Grants No. 42075160 and 41730962), Innovation Group Project of Southern Marine Science and Engineering Guangdong Laboratory (Zhuhai) (Grant No. 311021009), Guangdong Province Key Laboratory for Climate Change and Natural Disaster Studies (Grant No. 2020B1212060025), and National Key Scientific and Technological Infrastructure project “Earth System Science Numerical Simulator Facility” (EarthLab).

- Goudriaan, J. (1977). *Crop Micrometeorology: A Simulation Study*. Wageningen, Netherlands: Center for Agricultural Publishing and Documentation.
- Hagolle, O., Lobo, A., Maisongrande, P., Cabot, F., Duchemin, B., and De Pereyra, A. (2005). Quality Assessment and Improvement of Temporally Compositing Products of Remotely Sensed Imagery by Combination of VEGETATION 1 and 2 Images. *Remote Sensing Environ.* 94 (2), 172–186. doi:10.1016/j.rse.2004.09.008
- Hartley, A. J., MacBean, N., Georgievski, G., and Bontemps, S. (2017). Uncertainty in Plant Functional Type Distributions and its Impact on Land Surface Models. *Remote Sensing Environ.* 203, 71–89. doi:10.1016/j.rse.2017.07.037
- Haverd, V., Smith, B., Nieradzki, L., Briggs, P. R., Woodgate, W., Trudinger, C. M., et al. (2018). A New Version of the CABLE Land Surface Model (Subversion Revision R4601) Incorporating Land Use and Land Cover Change, Woody Vegetation Demography, and a Novel Optimisation-Based Approach to Plant Coordination of Photosynthesis. *Geosci. Model. Dev.* 11 (7), 2995–3026. doi:10.5194/gmd-11-2995-2018
- Holland, M. M., and Bitz, C. M. (2003). Polar Amplification of Climate Change in Coupled Models. *Clim. Dyn.* 21 (3–4), 221–232. doi:10.1007/s00382-003-0332-6
- Hovi, A., Raitio, P., and Rautiainen, M. (2017). A Spectral Analysis of 25 Boreal Tree Species. *Silva Fenn.* 51 (4), 1–16. doi:10.14214/sf.7753
- Jacquemoud, S., and Baret, F. (1990). PROSPECT: A Model of Leaf Optical Properties Spectra. *Remote Sensing Environ.* 34 (2), 75–91. doi:10.1016/0034-4257(90)90100-Z
- Ji, D., and Dai, Y. (2010). *The Common Land Model (CoLM) Technical Guide*. Beijing, China: GCESS, Beijing Normal University
- Kato, S., Loeb, N. G., Rose, F. G., Doelling, D. R., Rutan, D. A., Caldwell, T. E., et al. (2013). Surface Irradiances Consistent with CERES-Derived Top-Of-Atmosphere Shortwave and Longwave Irradiances. *J. Clim.* 26 (9), 2719–2740. doi:10.1175/jcli-d-12-00436.1
- Knorr, W., Schnitzler, K.-G., and Govaerts, Y. (2001). The Role of Bright Desert Regions in Shaping North African Climate. *Geophys. Res. Lett.* 28 (18), 3489–3492. doi:10.1029/2001gl013283
- Kovenock, M., and Swann, A. L. S. (2018). Leaf Trait Acclimation Amplifies Simulated Climate Warming in Response to Elevated Carbon Dioxide. *Glob. Biogeochem. Cycles* 32 (10), 1437–1448. doi:10.1029/2018gb005883
- Lawrence, D., Fisher, R., Koven, C., Oleson, K., Swenson, S., Vertenstein, M., et al. (2018). *Technical Description of Version 5.0 of the Community Land Model (CLM)*. Boulder, CO: National Center for Atmospheric Research, University Corporation for Atmospheric Research
- Lawrence, D. M., Fisher, R. A., Koven, C. D., Oleson, K. W., Swenson, S. C., Bonan, G., et al. (2019). The Community Land Model Version 5: Description of New Features, Benchmarking, and Impact of Forcing Uncertainty. *J. Adv. Model. Earth Syst.* 11 (12), 4245–4287. doi:10.1029/2018ms001583
- Levine, X. J., and Boos, W. R. (2017). Land Surface Albedo Bias in Climate Models and its Association with Tropical Rainfall. *Geophys. Res. Lett.* 44 (12), 6363–6372. doi:10.1002/2017GL072510
- Lukeš, P., Stenberg, P., Rautiainen, M., Möttöus, M., and Vanhatalo, K. M. (2013). Optical Properties of Leaves and Needles for Boreal Tree Species in Europe. *Remote Sensing Lett.* 4 (7), 667–676. doi:10.1080/2150704x.2013.782112
- Majasalmi, T., and Bright, R. M. (2019). Evaluation of Leaf-Level Optical Properties Employed in Land Surface Models. *Geosci. Model. Dev.* 12 (9), 3923–3938. doi:10.5194/gmd-12-3923-2019
- Malenovský, Z., Albrechtová, J., Lhotáková, Z., Zurita-Milla, R., Clevers, J. G. P. W., Schaepman, M. E., et al. (2007). Applicability of the PROSPECT Model for Norway Spruce Needles. *Int. J. Remote Sensing* 27 (24), 5315–5340. doi:10.1080/0143160600762990
- McGrath, M. J., Ryder, J., Pinty, B., Otto, J., Naudts, K., Valade, A., et al. (2016). A Multi-Level Canopy Radiative Transfer Scheme for ORCHIDEE (SVN R2566), Based on a Domain-Averaged Structure Factor. *Geosci. Model. Dev. Discuss.* 2016, 1–22. doi:10.5194/gmd-2016-280
- Middleton, E. M., and Sullivan, J. (2000). BOREAS TE-10 Leaf Optical Properties for SSA Species. Oak Ridge, Tennessee, USA: ORNL DAAC. doi:10.3334/ORNLDAAC/531
- Mottus, M., Sulev, M., and Hallik, L. (2014). Seasonal Course of the Spectral Properties of Alder and Birch Leaves. *IEEE J. Sel. Top. Appl. Earth Observations Remote Sensing* 7 (6), 2496–2505. doi:10.1109/jstars.2013.2294242
- Niu, G.-Y., Yang, Z.-L., Mitchell, K. E., Chen, F., Ek, M. B., Barlage, M., et al. (2011). The Community Noah Land Surface Model with Multiparameterization Options (Noah-MP): 1. Model Description and Evaluation with Local-Scale Measurements. *J. Geophys. Res.* 116, D12109. doi:10.1029/2010JD015139
- Pinty, B., Andredakis, I., Clerici, M., Kaminski, T., Taberner, M., Verstraete, M. M., et al. (2011). Exploiting the MODIS Albedos with the Two-Stream Inversion Package (JRC-TIP): 1. Effective Leaf Area Index, Vegetation, and Soil Properties. *J. Geophys. Res.* 116, D09105. doi:10.1029/2010jd015372
- Pu, B., and Dickinson, R. E. (2012). Examining Vegetation Feedbacks on Global Warming in the Community Earth System Model. *J. Geophys. Res.* 117, D20110. doi:10.1029/2012jd017623
- Qiu, B., Guo, W., Xue, Y., and Dai, Q. (2016). Implementation and Evaluation of a Generalized Radiative Transfer Scheme within Canopy in the Soil-Vegetation-Atmosphere Transfer (SVAT) Model. *J. Geophys. Res. Atmos.* 121 (20), 12145–12163. doi:10.1002/2016jd025328
- Randall, D. A., Wood, R. A., Bony, S., Colman, R., Fichet, T., Fyfe, J., et al. (2007). “Climate Models and Their Evaluation,” in *Climate Change 2007: The Physical Science Basis. Contribution of Working Group I to the Fourth Assessment Report of the Intergovernmental Panel on Climate Change*. Editors S. Solomon, D. Qin, M. Manning, Z. Chen, M. Marquis, K. B. Averyt, et al. (Cambridge, United Kingdom: Cambridge University Press).
- Rautiainen, M., Lukeš, P., Homolová, L., Hovi, A., Pisek, J., and Möttöus, M. (2018). Spectral Properties of Coniferous Forests: A Review of *In Situ* and Laboratory Measurements. *Remote Sensing* 10 (2), 207. doi:10.3390/rs10020207
- Sellers, P. J. (1985). Canopy Reflectance, Photosynthesis and Transpiration. *Int. J. Remote Sensing* 6 (8), 1335–1372. doi:10.1080/0143168508948283
- Soden, B. J., and Held, I. M. (2006). An Assessment of Climate Feedbacks in Coupled Ocean-Atmosphere Models. *J. Clim.* 19 (14), 3354–3360. doi:10.1175/JCLI3799.1
- Verrelst, J., Camps-Valls, G., Muñoz-Mari, J., Rivera, J. P., Veroustraete, F., Clevers, J. G. P. W., et al. (2015). Optical Remote Sensing and the Retrieval of Terrestrial Vegetation Bio-Geophysical Properties - A Review. *ISPRS J. Photogrammetry Remote Sensing* 108, 273–290. doi:10.1016/j.isprsjprs.2015.05.005
- Winton, M. (2006). Amplified Arctic Climate Change: What Does Surface Albedo Feedback Have to Do with it? *Geophys. Res. Lett.* 33 (3), L03701. doi:10.1029/2005gl025244
- Xue, Y., and Shukla, J. (1993). The Influence of Land Surface Properties on Sahel Climate. Part 1: Desertification. *J. Clim.* 6 (12), 2232–2245. doi:10.1175/1520-0442(1993)006<2232:TIOISP>2.0
- Yuan, H., Dickinson, R. E., Dai, Y., Shaikh, M. J., Zhou, L., Shangguan, W., et al. (2014). A 3D Canopy Radiative Transfer Model for Global Climate Modeling: Description, Validation, and Application. *J. Clim.* 27 (3), 1168–1192. doi:10.1175/jcli-d-13-00155.1
- Yuan, H., Dai, Y., Dickinson, R. E., Pinty, B., Shangguan, W., Zhang, S., et al. (2017). Reexamination and Further Development of Two-Stream Canopy Radiative Transfer Models for Global Land Modeling. *J. Adv. Model. Earth Syst.* 9 (1), 113–129. doi:10.1002/2016ms000773
- Zhai, J., Liu, R., Liu, J., Zhao, G., and Huang, L. (2014). Radiative Forcing over China Due to Albedo Change Caused by Land Cover Change during 1990–2010. *J. Geogr. Sci.* 24 (5), 789–801. doi:10.1007/s11442-014-1120-4
- Zhang, Y., Huang, J., Wang, F., Blackburn, G. A., Zhang, H. K., Wang, X., et al. (2017). An Extended PROSPECT: Advance in the Leaf Optical Properties Model Separating Total Chlorophylls into Chlorophyll a and B. *Sci. Rep.* 7 (1), 6429. doi:10.1038/s41598-017-06694-y

Conflict of Interest: The authors declare that the research was conducted in the absence of any commercial or financial relationships that could be construed as a potential conflict of interest.

Copyright © 2021 Dong, Yuan, Zhang, Li, Huang, Zhu, Peng and Dai. This is an open-access article distributed under the terms of the Creative Commons Attribution License (CC BY). The use, distribution or reproduction in other forums is permitted, provided the original author(s) and the copyright owner(s) are credited and that the original publication in this journal is cited, in accordance with accepted academic practice. No use, distribution or reproduction is permitted which does not comply with these terms.